

Deliverable D 3.4

Model of the multi-physic behaviour of refractory at high temperature

Document type **Deliverable D 3.4**

Document Version/ Status **1.7**

Primary Authors **Alain Gasser, alain.gasser@univ-orleans.fr, UORL**

Distribution Level **PU (Public)**

Project Acronym **ATHOR**

Project Title **Advanced THERmomechanical multiscale mOdelling of Refractory linings**

Grant Agreement Number **764987**

Project Website **www.etn-athor.eu**

Project Coordinator **Marc Huger, marc.huger@unilim.fr, UNILIM**
Alain Gasser, alain.gasser@univ-orleans.fr, UORL

Document Contributors **Eric Blond, eric.blond@univ-orleans.fr, UORL**
Sina Darban, darban@agh.edu.pl, AGH
Thaís Soares, thais.soares@civil.uminho.pt, UMINHO

History of Changes

Version	Date	Author (Organization)	Change	Page
1.0	07.09.2021	Sina Darban (AGH)	Introduction, defining system and variables	2-7
1.1	20.09.2021	Sina Darban (AGH)	Revision and correction the manuscript	2-9
1.2	18.10.2021	Thaís Soares (UMINHO)	Introduction, Application of multi-physics modelling for refractories, Revision	All
1.3	29/10/2021	Thaís Soares (UMINHO)	Application of multi-physics modelling for refractories, Revision	All
1.4	09/11/2021	Glyn Derrick (UNILIM) Marc Huger (UNILIM)	Final check	All
1.5	12/11/2021	Thaís Soares (UMINHO)	Revision	All
1.6	17/11/2021	Glyn Derrick (UNILIM)	English check	All
1.7	22/11/2021	Glyn Derrick (UNILIM) Marc Huger (UNILIM)	Final check	All

Table of contents

1 INTRODUCTION.....2

2 GENERAL ASPECTS REGARDING CORROSION OF REFRACTORIES3

3 THERMODYNAMICS OF IRREVERSIBLE PROCESSES FOR CORROSION4

3.1 Definition of system and state variables4

3.2 Thermodynamic conditions in modelling4

3.3 State variables4

3.4 Local state postulate5

3.5 Conservation laws5

3.6 First law of thermodynamics.....6

3.7 Second law of thermodynamics7

3.8 Chemical diffusion8

3.9 Chemical reactions and phase evolutions.....8

3.10 From entropy to state and evolution laws8

4 APPLICATION OF MULTI-PHYSICS MODELLING FOR REFRACTORY MATERIALS.....9

4.1 Model of a glass melting tank10

4.2 Model of a membrane wall gasifier10

4.3 Model of an entrained-flow gasifier.....11

4.4 Corrosion of MgO-C refractory.....12

4.5 Model of a black liquor gasifier.....13

4.6 Application of thermodynamics of irreversible processes for corrosion.....14

5 CONCLUSION19

6 REFERENCES.....19

1 Introduction

Refractories are advanced materials that can sustain operation conditions at temperatures typically above 1000 °C, making them key enablers in the production of essential common products such as glass, cement and steel. The response of refractory materials to in-service conditions is a complex subject to study, several factors influence and increase the difficulty in predicting real world behaviour. Refractories represent a class of materials with intricate characteristics, that vary greatly with the chemical elements involved and its manufacturing process. Then, there is the application in the industrial field, where the materials are exposed to extremely high temperatures and corrosive environments. These factors together, lead to the necessity of utilising a multi-physics approach to determine the performance of the materials. To create structures that are safe to use, efficient and with the longest lifetime possible, a mechanical assessment of the structure’s response is needed. In order to do so, mechanical characteristics are required. However, exposure to corrosive environments and high-temperature alters these mechanical characteristics. Thus, experimental tests in different scenarios become essential. The amount of data demanded increases, and also the complexity of the experiments. As such, data that is currently available in the literature is focussed on a few very specific cases. Furthermore, the mathematical base necessary to translate and connect all these subjects requires a broad background and may be seen as confusing.

The ATHOR project has sort to advance this new area of science by bringing together materials, corrosion and multi-physics scientists to expand frontier knowledge regarding particular responses of refractories, the experimental data available and numerical representations of refractory responses at different scales. As with all cutting-edge technologies, the fundamentals need to be developed accurately, over time, to provide the platform for future breakthroughs. This report will present modelling approaches that can describe the evolution of the thermomechanical behaviour linked to refractory corrosion and that can be numerically implemented and solved. First, a general description of the corrosion problem in refractories will be presented, followed by the definition of a set of equations able to synthesize this behaviour (constitutive equations, transport, simplified chemical reactions). And finally, some examples from state of art research will be presented.

2 General aspects regarding corrosion of refractories

Refractories are of great interest for energy intensive industries, such as the iron and steel industry, due to their capacity to protect metallic structures and equipment from high temperatures and aggressive working environments. During service, these materials are exposed to thermal gradients often coupled with a reactive chemical environment that might induce corrosion [1], [2]. To consider the effect of all these complex service conditions on the refractory material, the application of multi-physics modelling via numerical studies becomes necessary.

Corrosion of refractories can be defined as refractory wear by change of mechanical properties and loss of thickness and mass from the exposed face of the refractory as a consequence of chemical attack. This chemical attack, a process in which the refractory and the corrosive liquid react, approaches a chemical equilibrium in the zone of contact between the refractory and the liquid [1]. Refractory corrosion involves a combination of different mechanisms, such as dissolution and invasive penetration, where diffusion, grain boundary, and stress corrosion may all be present. Oxidation-reduction reactions, where absorption, desorption, and mass transport phenomena also come into play, generally under pressure and temperature gradients [3][4].

Refractories are heterogeneous, multiphase materials, consisting of crystallites, glassy phases and pores all of different sizes. Each crystalline constituent has a different degree of purity, depending upon its specific preparation and thermal history before use. The grain morphology also varies, as well as the grain size distribution, with its inherent porosity between grains [3]. On top of the variation in composition of the materials, several different processes can take place during corrosion, as such, a simple, all-encompassing general theory of refractory corrosion does not exist [5][3]. This implies that corrosion is a system property rather than a simple material one [6], and that corrosion resistance of a refractory material is not an intrinsic property of such a product, but at best an indication of a process intensity, where many parameters need to be defined to appreciate the significance of such a characteristic [3].

According to the chosen modelling approach, the predictions for the mechanical stress field in the refractory linings can vary greatly. Even though real stress values are somewhat difficult to obtain, it is known that purely thermoelastic predictions are inaccurate due to the material's evolution with temperature and chemical environments [2]. Hence, the design of refractory linings represents an engineering challenge that requires a broad background both in material engineering and thermomechanical structural design [2]. Conventionally, the design of refractory linings is based on thermal computations and simplified thermomechanical considerations, together with some knowledge on thermochemistry and practical know-how, such as that summarized by Schacht [1]. Temperature fields from numerical analysis or measurements from real plants are used as imposed loads in thermomechanical simulations. Consequently, the stress fields obtained may represent the initial state of a new structure, before the interaction between chemistry and mechanics take place [2].

The local values of the temperature field are used in corrosion studies to select suitable material for linings that are in danger of corrosion. Furthermore, it is essential to understand the corrosion to approach the appropriate material's composition for each zone (slag line, working line, etc.). Even though the corrosion problem is strongly connected to the thermomechanical design of the structure, coupling thermomechanical and thermochemistry modelling is not the norm. Usually, in the best-case scenario, these two points are studied sequentially and sometimes, iteratively. As shown in **Figure 1**, coupling the thermomechanical behaviour to the corrosion and phase change is possible thanks to broader information regarding the corrosion, refractories and developments in the computational capacities for simulations [2].

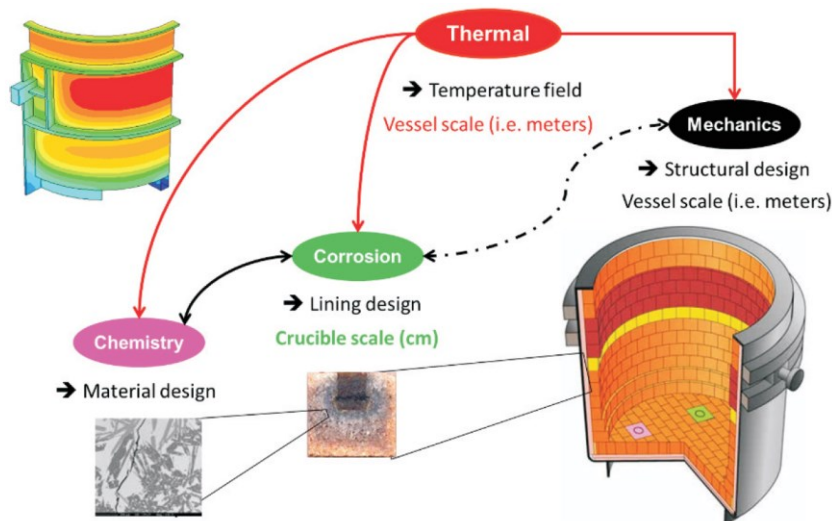


Figure 1: Refractory lining design; a multiscale and multi-physics problem [2].

3 Thermodynamics of irreversible processes for corrosion

Writing a multi-physics model by simply listing the laws of physics is not always sufficient or relevant. Indeed, this approach leads, more often than not, to the consideration of only the evolution of the coefficients of the state laws with state variables. In this section, a theoretical basis will be presented to help understand the types of multi-physics modelling that are currently being developed that are applicable to corrosion, phase changes, and mechanical behaviour. The following subsections will present the Thermodynamics of Irreversible Processes (TIP), which is a strong framework able to model this coupling between thermochemistry and thermomechanics in fields such as geology and mechanics, and has been presented in detail in [2].

3.1 Definition of system and state variables

The first step in the development of a model is the proper definition of the system, its geometrical boundaries, the level of representation, the physics that play the most important roles and the related state variables. For refractories, this is complicated due to the complexity of the microstructure and the number of phenomena involved to describe the material evolution. Furthermore, according to the objective, it might be necessary to include part of the encompassing environment to define the boundary conditions. As the framework proposed in this section has the aim of helping engineers design industrial vessels and identify key parameters regarding the applications, refractories are assumed to be a continuous porous medium without any description of the microstructure. The parcel of refractory corresponds to a "Representative Elementary Volume", in which all the phases are represented by average values and are superimposed in each point.

3.2 Thermodynamic conditions in modelling

By definition, the equilibrium condition in a thermodynamic system is achieved when the internal energy is at the lowest level or entropy is at the highest level. The third thermodynamic principle, states that equilibrium defined by minimization of energy or maximization of entropy, are equal if the temperature is strictly positive. Moreover, the minimum internal energy represents the final state in equilibrium condition, and maximum entropy is considered as a way of evolution from the initial stage to the final stage. Finally, the steady state might be defined as a condition between equilibrium and evolution that requires external energy to be continued. Since most of the industrial systems are operated close to a "stationary" regime; it is assumed that industrial operations are in a steady-state condition.

3.3 State variables

The description of the system and its evolution must be represented by a reasonable selection of state variables. A good selection corresponds to the minimum number of independent parameters needed to describe the system and its evolution. Commonly, the number of variables depends on the number of physics that need to be accounted for, the choice of the variables and their type is arbitrary. In the case of refractory materials, with physical properties that depend on the temperature cycle, some simple state variables could not be considered as the best set of variables due to the "history effect". Therefore, the best way to describe the complex evolutions of dynamic system is to implement extensive variables. Nevertheless, before selecting the sets of variables, it is necessary to study all available experimental data to identify the primary mechanism and the evolution process in the system to associate that with set of thermodynamic variables.

Defining "extensive parameters" of the system in order to establish an acceptable model occurs by defining the measurable parameters that correspond to the thermodynamic system. Furthermore, finding suitable thermodynamic potential (Gibbs, Helmholtz, etc.) represents another requirement in this regard. Finally, the choice of state variables comes from the compromise between the physics, measured data available and the objective of the model. **Table 1** summarizes the state variables that are currently used for the four-major physics in the refractory field.

Table 1: Example of basic state variables for classical physics in the refractory field.

	Extensive state variable	Intensive state variable		
		Associated densities		
Mechanics	Volume Ω	Second rank strain tensor $\underline{\underline{\xi}}$	Second rank stress tensor $\underline{\underline{\sigma}}$	Total pressure P mechanical force
	Displacement \vec{U}			
Chemical reaction phase change	Extent $d\xi = \frac{dN_i}{v_i}$	Volume extent $\frac{\xi}{\Omega}$	Volume affinity $\hat{A} = -\sum_i V_i \frac{\rho_i}{M_i} \mu_i$	Chemical affinity $A = -\sum v_i \mu_i$
Chemical diffusion	Number of moles N_i	Volume concentration C_i	Volume chemical potential $\hat{U}_i = \frac{\rho_i}{M_i} \mu_i$	Chemical potential μ_i
Fluid transport (porous media)	Fluid mass M_f	Fluid mass density $\rho_f = \frac{M_f}{\Omega}$	Specific pressure $\frac{p}{\rho_f}$	Pore pressure, interstitial pressure p

3.4 Local state postulate

Usually, the equilibrium state in thermodynamics is defined by the knowledge of the values of the state variables. The “local state postulate” is implemented to move from the thermostatic (prediction and description of equilibrium) to thermodynamic approach (the description and prediction of evolution, not only the initial and final state). It states that the evolution is locally a succession of equilibrium. Hence, in an evolving system, the thermodynamic state of variables is represented by the same variables as the equilibrium, despite their evolution rate. From a modelling point of view, the main interest is to distinguish the variables that characterize an irreversible evolution of the system from the other variables. Consequently, there is no interest in dividing the variables into internal or external ones [7].

3.5 Conservation laws

The balance of the extensive quantity, such as mass, momentum and energy, can be computed considering the given domain and its surrounding environment. This will lead to the definition of continuity equation established when the quantity is not conservative, as entropy. For each extensive independent parameters X contained in a closed Ω volume of boundary $\partial\Omega$, so the balance of X can be written as:

$$\frac{dX}{dt} = \frac{d}{dt} \int_{\Omega} x d\Omega = - \int_{\partial\Omega} \vec{J}_x \cdot \vec{n} dS + \int_{\Omega} r_x d\Omega \quad \text{Equation 1}$$

Where x is the volume density of X , \vec{J}_x is the local density of the flux of X through the surface $\partial\Omega$ of the volume Ω and r_x is the local volume density of source X . Considering the material derivative rule, the first derivative could be written as:

$$\frac{d}{dt} \int_{\Omega} x d\Omega = \int_{\Omega} \frac{\partial x}{\partial t} d\Omega + \int_{\Omega} \overrightarrow{grad}_M(x) \cdot \vec{V}_{R_0}^M d\Omega + \int_{\Omega} x \text{div}(\vec{V}_{R_0}^M) d\Omega \quad \text{Equation 2}$$

Where $\vec{V}_{R_0}^M$ is the velocity of the considered point M in Ω with regards to a chosen referential, \overrightarrow{grad}_M is the gradient around M and div represents the divergence. The two first terms of the right-hand side of the equal sign correspond to the particle derivative of x while the last one corresponds to the derivative regarding the time of the elementary volume. Hence, using the Stokes theorem, the local form of the balance equation is:

$$\frac{\partial x}{\partial t} + \text{div}(x \vec{V}_{R_0}^M) - r_x = -\text{div} \vec{J}_x \quad \text{Equation 3}$$

The left side of **Equation 3** corresponds to the fluctuation inside the volume, while the right side represents the balance of the exchange with outside. From the left, the first term represents the local rate of change of the density of X , the second term represents the convective term accounting for local transport of X inside the domain, and the third term is the density of the internal source of X . On the right-hand side, the term represents the balance of the exchanges of X with the outside of the domain. The **Equation 3** could be written in a simple form as:

$$\frac{\partial x}{\partial t} = r_x - \text{div}(x\vec{V}_{R_0}^M + \vec{J}_x) \quad \text{Equation 4}$$

Hence, the rate of density alteration is equal to the sum of the source term and the balance of fluxes. According to the physical properties (thermal, chemistry, mechanical, etc.), the extensive variables are not the same, even for the fluxes and sources, but the balance **Equation 4** is always the same.

Table 2 shows the associated densities, fluxes, and sources for the main physics in the refractory field. Not all these terms were defined at this stage of the report. Nevertheless, these terms shall be used and explained in the following sections.

Table 2: The terms of the balance for different extensive state variables

Extensive parameter	Density	Flux	Source
Mass	ρ	0	0
Fluid mass	$m_f = \rho_f S\phi$	$\vec{M} = \rho_f S\phi \vec{V}_r$	$\dot{m}_{s \rightarrow f} + \dot{m}_{f \rightarrow g}$
Momentum	$\rho \vec{V}$	$\underline{\underline{\sigma}}$	$\rho \vec{g}$
Mole of solute	ρx_i	$\vec{J}_i + \rho x_i \vec{V}$	$\sum_i V_{ij} M_i \left(\frac{\xi_r}{\Omega} \right)$
Internal energy	ρe	$\vec{q} + \sum_i \frac{h_i}{M_i} \vec{J}_i$	$\underline{\underline{\sigma}} : \underline{\underline{\xi}} + \sum \vec{g} \cdot \vec{J}_i + r$
Entropy	ρs	$\frac{\vec{q}}{T} + \sum_i \frac{1}{M_i} \frac{h_i - \mu_i}{T} \vec{J}_i$	≥ 0

3.6 First law of thermodynamics

The first law of thermodynamics assumes that there is conversion of the total energy of a closed system. However, refractories should be considered as open systems, as there might be slag impregnation or gas diffusion through porosity. From the classical global point of view, it leads to:

$$\frac{d}{dt}(U + K) = P_{ext} + Q + \dot{\xi} \quad \text{Equation 5}$$

Where U is the internal energy, K is the kinetic energy, P_{ext} the mechanical power of the external load, Q the heat power and $\dot{\xi}$ the time derivate of the balance of energy exchange with the surrounding environment - the upper point denotes the time derivative. The power of the energy exchange is correlated to the energy transport by mass flow across the boundary of the system in one second, without the power for establishment or maintenance of the flow through the boundary. It corresponds to the definition of the enthalpy flux:

$$\dot{\xi} = - \sum_i \int_{\partial\Omega} \frac{h_i}{M_i} \vec{J}_i \cdot \vec{n} dS \quad \text{Equation 6}$$

Where h_i is the molar enthalpy of species i and M_i is the molar mass of species i , $\vec{J}_i = \rho_i \vec{V}_i$ is the volume density of the mass flux of species i with ρ_i the partial density of species i and \vec{n} is the local normal to the boundary. The minus sign comes from the convections: an entrance flux is positive, but the normal is oriented to the outward of the medium. By using the appropriate densities, the first principle (**Equation 5**) leads to:

$$\frac{d}{dt} \int_{\Omega} \rho e d\Omega + \frac{d}{dt} \int_{\Omega} \frac{1}{2} \rho (\vec{V}^M)^2 d\Omega = \int_{\Omega} \vec{T}(M, \vec{n}) \cdot \vec{V}^M dS + \int_{\Omega} \rho \vec{g} \cdot \vec{V}^M dS + \int_{\Omega} r d\Omega - \int_{\partial\Omega} \vec{q} \cdot \vec{n} dS - \sum_i \int_{\partial\Omega} \frac{h_i}{M_i} \vec{J}_i \cdot \vec{n} dS \quad \text{Equation 7}$$

Where ρ is the mass density of the system, e is the specific internal energy, \vec{V}^M is the velocity of the considered point M in the domain Ω , $\vec{T}(M, \vec{n})$ is the stress vector, \vec{g} is the gravity field, \vec{q} the local density of heat flux and the local density of heat source. Considering the definition of the Cauchy stress tensor ($\vec{T}(M, \vec{n}) = \underline{\underline{\sigma}}(M) \cdot \vec{n}$, where $\underline{\underline{\sigma}}$ is the second rank Cauchy stress tensor, and the concentration rule, **Equation 7** becomes:

$$\frac{d}{dx} \int_{\Omega} \rho \left(e + \frac{1}{2} (\vec{V}^M)^2 \right) d\Omega = \int_{\partial\Omega} \left(\underline{\underline{\sigma}} \cdot \vec{V}^M - \vec{q} - \sum_i \int_{\partial\Omega} \frac{h_i}{M_i} \vec{J}_i \right) \cdot \vec{n} dS + \int_{\Omega} (\rho \vec{g} \cdot \vec{V}^M + r) d\Omega \quad \text{Equation 8}$$

Therefore, the evolution rate of the total energy in the domain results from the work, thermal, enthalpy fluxes and the balance of the work and heat sources. Using the divergence theorem, the operator's concentrations rules, derivation rules, and the momentum balance, the total form of the first law becomes:

$$\rho \dot{e} = \underline{\underline{\sigma}} : \underline{\underline{\dot{\varepsilon}}} - \text{div} \vec{q} + r - \text{div} \left(\sum_i \frac{h_i}{M_i} \vec{J}_i \right) \quad \text{Equation 9}$$

Where $\underline{\underline{\varepsilon}}$ is the second rank strain tensor.

A phase evolution does not affect the total internal energy of the system; it might only induce conversion of the internal energy. In the second law of thermodynamics, this aspect will be considered. However, it does not affect the first law of thermodynamics. Regarding the case of a porous medium subjected to flux diffusion through its porous structure, the first principle should be written considering both solid and fluid phases. Hereafter, the case of a porous solid totally filled with one fluid will be presented. Therefore, the first principle for a saturated porous medium is written as:

$$((1 - \Phi) \rho_s + \Phi \rho_f) \dot{e} = \underline{\underline{\sigma}} : \underline{\underline{\dot{\varepsilon}}} + \rho_f \Phi \vec{V}_r \cdot (\vec{g} - \vec{\gamma}_f) + \text{div}(h_f \rho_f \Phi_f - \vec{q}) + r \quad \text{Equation 10}$$

Where subscript s refers to the solid skeleton and subscript f refers to the fluid phase, Φ is the volumetric porosity, $\vec{\gamma}_f$ the absolute acceleration of the fluid and \vec{V}_r is the relative velocity of the fluid regarding the solid skeleton. The specific enthalpy of the fluid is equal to the specific internal energy of the fluid plus the specific pressure:

$$h_f = \frac{p}{\rho_f} + e_f \quad \text{Equation 11}$$

Where p is the pore pressure of the fluid inside the porosity and e_f is the specific internal energy of the fluid.

3.7 Second law of thermodynamics

The second law of thermodynamics introduces the concept of irreversible reactions or natural reactions (i.e. heat is transferred from the hot spot to the cold spot and not vice versa). The difference between the first and second laws of thermodynamics is in the concept of them. While in the first law, the quantitative conservation of energy is presented, in the second law of thermodynamics, the qualitative degradation of energy produced by transformation, is introduced. It should be taken into account that it is impossible to transform all the energy into mechanical work. Hence, the second thermodynamic law represents the asymmetry of energy conversions, and therefore involves a time scale. Based on Carnot's theory [8], entropy is the energy used to increase the temperature by 1 K in one second, or in other words, it is the necessary power for the system's evolution. The entropy rate could be written as:

$$\dot{S} = \sum_i \left(\frac{\partial S}{\partial X_i} \right)_{X_j} \dot{X}_i \quad \text{Equation 12}$$

Where S is the entropy and X_i represents the extensive state variables. The flux could be defined as:

$$J_i = \dot{X}_i \quad \text{Equation 13}$$

Based on the definition of entropy (consumed energy to increase the temperature), it is helpful to define the thermodynamic force, which is called affinity, as:

$$F_i = \left(\frac{\partial S}{\partial X_i} \right)_{X_j} \quad \text{Equation 14}$$

As a result, the entropy ratio is the amount of the product of every flux by its related force, and it matches to a power:

$$\dot{S} = \sum_i F_i J_i \quad \text{Equation 15}$$

Hence, the entropy rate can be expressed if the extensive associate variables are identified. In the sequence, the evolution might be derived, and subsequently the coupling effect. In order to illustrate this approach, two specific cases of phenomenon that take place in refractory materials will be presented: chemical diffusion and chemical reaction.

3.8 Chemical diffusion

In the heterogeneous system, the first natural evolution trend is the diffusion of chemical species, which is an irreversible phenomenon. A reasonable extensive state variable linked to the mass of diffused species (i) is the number of moles, N_i . Thus, the entropy ratio of a multi-component system would be defined as:

$$\dot{S} = \sum_i \left(\frac{\partial S}{\partial N_i} \right)_{T,P,N_j} \dot{N}_i \quad \text{Equation 16}$$

According to [9], the molar chemical potential could be written as:

$$-\frac{\mu_i}{T} = \left(\frac{\partial S}{\partial N_i} \right)_{T,P,N_j} \quad \text{Equation 17}$$

Based on **Equation 17**, the entropy flux can be rewritten as:

$$\dot{S} = \sum_i -\frac{\mu_i}{T} \dot{N}_i \quad \text{Equation 18}$$

3.9 Chemical reactions and phase evolutions

Chemical reactions and phase evolution are inevitable during the diffusion of chemical components of flux in the microstructure, and there is a possibility to characterize the phase evolution and chemical reactions thermodynamically [10]. The new phase could be considered as a new species, and the reaction could be written as:



The capital letters show a chemical species and a phase or a molecule depending on the target reaction. The mass balance of a reaction could be written as:

$$\sum_i V_{ir} M_i = 0 \quad \text{Equation 20}$$

Where M_i is the molar mass of component i , and the stoichiometric coefficient V_{ir} are positive for a product and negative for the reactant. Index i shows the component while index r represents the reaction. Similar to the chemical diffusion, the entropy ratio could be written like **Equation 18** because the extensive variables are related to a chemical reaction which involves species i is the number of moles, N_i . Hence, similar to the chemical diffusion process, the entropy rate is:

$$\dot{S} = \sum_i -\frac{\mu_i}{T} \dot{N}_i \quad \text{Equation 21}$$

The mole numbers of the reactants and products change through the phase change and are linked together by the stoichiometric coefficients. Afterwards, to characterize the evolution of the transformation, the extent ξ_r of reaction r can be written as:

$$d\xi_r = \frac{dN_i}{V_{ir}} \quad \text{Equation 22}$$

V_{ir} is the stoichiometric coefficient of the i -th species in the r -th reaction; the entropy could be written as:

$$\dot{S} = \sum_{i,r} -\frac{V_{ir} \mu_i}{T} \dot{\xi}_r \quad \text{Equation 23}$$

3.10 From entropy to state and evolution laws

The basics of TIP are to derive the evolution law from the Clausius-Duhem relationship which accounts for the first and second laws. This inequality includes energy conservation and degradation.

For refractories, the general domain is an open reactive porous continuous media, filled with liquids and gases, with a complex microstructure that evolves by phase changes and chemical reactions. Broad knowledge of physics is needed to create a detailed model of such a complex medium, however, it is possible to use a simpler approach and obtain good results. This approach considers an open continuous reactive medium at the macroscopic scale, without consideration of the microstructure.

Entropy is an extensive state variable, the entropy balance can be written in its local form as:

$$\rho \dot{s} = -\operatorname{div} \vec{J}_s + r_s \quad \text{Equation 24}$$

Where \dot{s} is the time derivative of the specific entropy, \vec{J}_s is the entropy flow and r_s is the entropy source of the system. The bulk density ρ represents the average density of the whole system. The second law imposes that the source term can only be positive or null. Hence, the fundamental inequality corresponds to:

$$\rho \dot{s} + \operatorname{div} \vec{J}_s \geq 0 \quad \text{Equation 25}$$

The entropy flow is equal to the heat flow divided by the absolute temperature plus the difference between the enthalpy flow and the free enthalpy flow in each source. Considering Gibbs' law, the free enthalpy is equal to the chemical potential, and so:

$$\vec{J}_s = \frac{\vec{q}}{T} + \sum_i \frac{1}{M_i} \frac{h_i - \mu_i}{T} \vec{J}_i \quad \text{Equation 26}$$

Where $\vec{J}_i = \rho_i \vec{V}_i$ is the mass flux of species i and M_i is the molar mass of species i .

It is interesting to note the analogy between the case proposed here and the case of the fluid flux. This rigorous analogy established the equivalence between the molar chemical potential and the specific pressure p/ρ_f (see [Equation 11](#)). Therefore, the chemical potential might be seen as the work needed to add one more mole to a rigid domain at constant temperature. Thus, the chemical potential is the driven force of mass diffusion, such as pressure for fluid.

Considering the first principle, the following can be written as:

$$\rho \dot{e} = \underline{\underline{\sigma}} : \underline{\underline{\varepsilon}} + r - \operatorname{div} \left(\vec{q} + \sum_i \frac{h_i}{M_i} \vec{J}_i \right) \quad \text{Equation 27}$$

Moreover, considering that r is the heat source from physics that takes place in the bulk, and accounting for the entropy definition [Equation 15](#), it can be written as:

$$r = \sum_j \vec{F}_j \vec{J}_j \quad \text{Equation 28}$$

Where \vec{F}_j is the volume force and \vec{J}_j a flux species. However, this source term will be neglected in what follows. This is because, in the refractories field, it is considered reasonable to neglect other types of physics than thermal, chemical, and mechanical. Thus, considering the mass balance of each species, it reads:

$$\rho \dot{x}_i = -\operatorname{div} \vec{J}_i + \sum_r v_{ir} M_i \left(\frac{\xi_r}{\Omega} \right) \quad \text{Equation 29}$$

The fundamental inequality becomes:

$$\rho (T \dot{s} - \dot{e}) + \underline{\underline{\sigma}} : \underline{\underline{\varepsilon}} + \sum_i \frac{\rho \mu_i}{M_i} \dot{x}_i + \sum_r \frac{A_r \xi_r}{\Omega} + T \vec{q} \overrightarrow{\operatorname{grad}} \left(\frac{1}{T} \right) - \sum_i \vec{J}_i \cdot \overrightarrow{\operatorname{grad}}_T \left(\frac{\mu_i}{M_i} \right) \geq 0 \quad \text{Equation 30}$$

Where $\overrightarrow{\operatorname{grad}}_T$ denotes the gradient considering a homogenous temperature field.

[Equation 30](#) accounts both for the first and second principle of thermodynamics, the energy balance and the mass balance, and it is known as the Clausius-Duhem fundamental inequality. This equation merges all the conditions that a medium must follow from the thermodynamic point of view and exhibits six different origins for the entropy rate of the system. According to the terms of [Equation 30](#), from left to right, the possible dissipation forms are the conversion of internal energy to heat; the mechanical load; the mass title change; the chemical reactions or phase changes inside the system; the heat exchange/flux; and finally, the mass exchange/flux. Depending on the problem, the importance or necessity of each term varies. Furthermore, the different hypotheses might lead to different evolution laws. Nevertheless, this equation represents a general base from which several multi-physics problems might be modelled.

4 Application of multi-physics modelling for refractory materials

In this section, several studies regarding numerical modelling of refractories' corrosion will be presented. It will become clear that even though a complete framework on the mathematical modelling of corrosion in refractories was presented in the previous section, several works found in the literature about this subject do not use this coupled approach. Instead, they focus on localized problems that are described by empirical equations that define the wear rate of the material, for example, and propose a link

between mass and heat transfer, but not to the mechanical aspect of the problem. Herein, both types of approaches will be presented.

4.1 Model of a glass melting tank

Nishikawa et al. [11] developed a one-dimensional numerical model to predict long-term refractory corrosion of a glass melting tank, by means of higher accuracy treatment for radiative heat transfer. Rosseland's approximation is a popular method to calculate the radiative heat transfer in glass melts. However, even though the method provides good agreement for optically thick mediums such as glass melts, it is not considered to be reliable near the boundary because the radiation from it is neglected in the approximation concept. Thus, the exponential integral method which is a high accuracy expression for radiative heat transfer is introduced in order to evaluate the temperature on the glass-refractory boundary. The model predicts the corrosion rate at the flux line which is one of the critical parts in determining the lifetime of a tank. Since it is unsuitable for manufacturing requirements to consider the all-physical mechanisms in the simulation, the authors have proposed a simple one-dimensional simulation model by considering the temperature of the side tank block above the flux line as the fixed temperature boundary condition and solving the moving boundary heat transfer by refractory corrosion without thermal convection. The verification of this numerical model is made by the comparative investigation with ordinary reference data of refractory corrosion in melting tanks.

The analytical and numerical models proposed in Nishikawa et al. [11] study are schematically represented in **Figure 2**. In the analytical one, heat transfer and the moving boundary are taken into account, and thermal convection is not considered in the concave area caused by refractory corrosion. The numerical model is assumed to be a one-dimensional thermal radiation and conduction heat transfer model in a simplification of the several complex mechanisms of refractory corrosion.

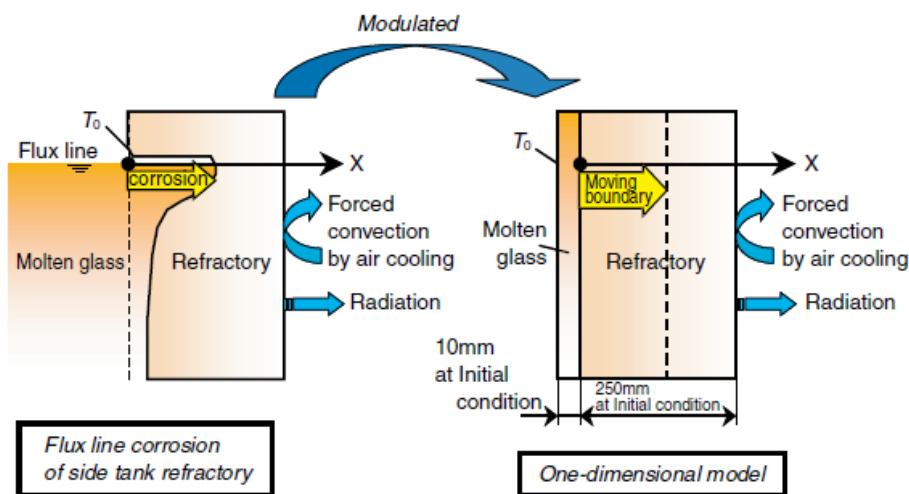


Figure 2: Schematic of the analytical model representing a fraction of the glass melting tank wall at the flux line: the analytical model on the left side and numerical on the right side [11].

The mathematical model is formed by the equation for transient heat transfer together with the equation of mass transfer, responsible to represent the occurrence of corrosion. The main corrosion process adopted in this study is related to the solubility of the refractory with dependence on its temperature. To represent this process, the diffusion coefficient of refractory in molten glass is assumed to be Arrhenius type expression. The two primary equations are solved in sequence for the one-dimensional domain, first the temperature problem then the mass transfer, which gives as results the distance of the moving boundary due to refractory corrosion. The prediction result is in good agreement with the reference corrosion rate. Finally, the model can be applied to investigate the way of extending the lifetime for a melting tank refractory.

4.2 Model of a membrane wall gasifier

Zhang et al. [12] studied the slag behaviours on the top cone of gasifiers to assess the refractory wall corrosion and safe operation in a membrane wall gasifier. An entrained-flow gasifier can be divided into several types, as shown in **Figure 3**. In all of them, the top of the gasifier represents an important area, which helps to collect the syngas, reduces the backflow area, or increases the structural strength. The usual shape is a cone or a dome, and it generally consists of a liquid slag layer, a solid slag layer, a refractory wall, a metal wall, and cooling water. The slag behaviours and characteristics of the top cone section have a vital influence on the design of this area. For instance, the heat transfer rate of the slag layer on the top cone will determine the arrangement of cooling-water pipes and the cone angle. The slag layer thickness distribution will determine the heat flux density

on the top cone and refractory wall temperature and service lifetime. Moreover, gasifiers often encounter the problem of refractory wall corrosion on the upper section, which will increase the production costs and threaten the gasifier safety in severe cases. Therefore, it is necessary to study the slag behaviours on the top cone of gasifiers.

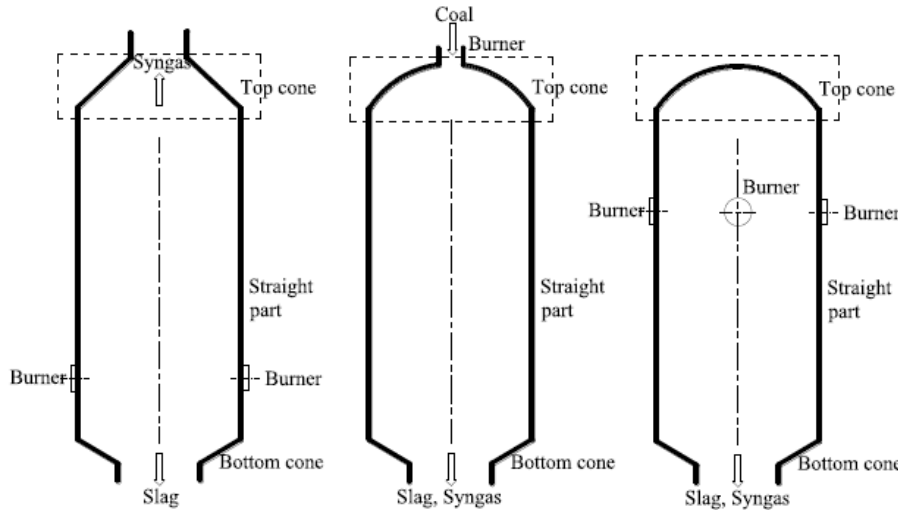


Figure 3: Gasification chamber structure diagram of several typical entrained-flow gasifiers: Shell gasifier; GE gasifier; and OMB gasifier, respectively [12].

Zhang et al. [12] proposed a steady-state slag flow and heat transfer model on the top cone of a shell gasifier, illustrated in Figure 4. The model was established based on some governing equations about mass, momentum, and energy conservation. Generally, high-temperature corrosion of the SiC refractory wall includes physical abrasion, oxidation corrosion, and metal ion erosion in the molten slag. However, the surface of refractory materials in a membrane wall entrained-flow gasifier is basically covered with a solid slag layer. Thus, refractory materials are less likely to be eroded by physical abrasion and metal ions, and the quality will not be reduced after metal ion erosion. Therefore, only oxidation corrosion was considered in this study. Since the reaction rate was considered to be slow, the mass loss rate of SiC was expressed using chemical reaction kinetics. Finally, the slag behaviour characteristics were obtained by solving the equations, and the variation trends with the cone angle and the location from the top outlet of the gasification chamber were shown. Modelling results included the slag thickness distribution, slag RTD, heat flux density distribution, and SiC refractory wall surface temperature distribution. The results showed differences in the slag thickness and the heat flux density between the top and the bottom of the cone. Moreover, the influence of the cone angle on the slag thickness and the heat flux density was also studied. Furthermore, the obtained results showed that the refractory wall surface temperature and the linear corrosion rate significantly increased while the gas temperature increased. Hence, the operating temperature should be kept in control to extend the refractory wall lifetime and ensure the gasifier safety.

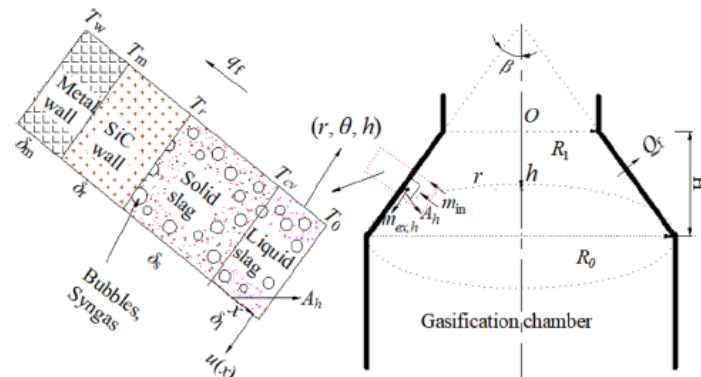


Figure 4: Schematic diagram cross-section of the top cone region in the gasification chamber: layers distribution with definition of temperature, thickness, heat and mass flux. [12].

4.3 Model of an entrained-flow gasifier

In another study about entrained-flow gasifiers, Lin et al. [13], built comprehensive models of slag flow and refractory bricks heat transfer. Even though there are many studies [14],[15],[16] into the corrosion characteristics of refractory bricks using the thermodynamic model, theoretical models regarding the effect of operating conditions on refractory brick corrosion from the perspective of liquid-solid diffusion are rare. Refractory brick corrosion can be regarded as a liquid-solid diffusion mechanism:

liquid slag continuously impacts the surface of the refractory brick and penetrates its interior. Concerning the operation of a commercial gasifier, it is important to understand the corrosion mechanism to improve the service life of the refractory brick and provide guidance for its installation. Therefore, a series of models including the Endell model, as well as internal and external diffusion models were built to simulate the corrosion state of refractory brick from the perspective of the liquid–solid phase diffusion mechanism.

A top single-burner down-flow gasifier was chosen as the model for the studies proposed by Lin et al. [13]. The gasifier wall was divided into a series of control cells along the axial direction, and the slag flow in the control cell is shown in **Figure 5**. In order to investigate the molten slag flow and heat transfer characteristics, mass, momentum, and energy equations were proposed.

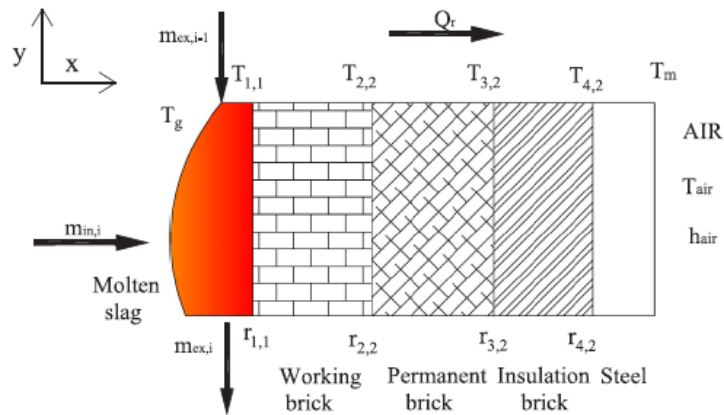


Figure 5: Schematic of the control cell representing the gasifier wall: layers distribution with definition of temperature, thickness, heat and mass flux [13].

The corrosion of refractory bricks was studied by Lin et al. [13] using a specific coal ash with stable compositions and a chromia-alumina-zirconia refractory. Therefore, only the influence of operating conditions on the corrosion rate was investigated. The reaction kinetics of the refractory brick corrosion were considered to be related to the constant terms in each model. Three different models were used to define the corrosion process. The Endell model, which is a semi-empirical model, predicts the refractory brick corrosion rate based on the slag viscosity, brick surface temperature, and slag mass outflow rate. However, as it does not explain the corrosion mechanism of refractory bricks, more comprehensive models were proposed in the paper to describe the corrosive process. One of them was the internal diffusion model, which establishes corrosion rate as a function of the pore diameter, slag surface tension, contact angle, and slag viscosity. Another one, the external diffusion model, considers the influence of the external diffusion of reaction species formed by the reaction between the slag and the refractory. The results from these types of reactions might form a layer that acted as a barrier to block molten slag infiltration into the bulk refractory, and consequently limits brick corrosion.

The flow characteristics of slag and the heat transfer of the refractory brick, including the brick surface temperature, slag thickness, slag velocity, metal wall temperature, and brick corrosion were calculated from the defined equations with the help of Matlab software. All the non-linear equations in this study were solved by the least squares method and the definite integral were solved by Simpson's 1/3 rule of integration. The output of the slag flow and heat transfer model includes the slag temperature, slag velocity, slag thickness, the temperature profile of the different layers and the heat loss. Moreover, the slag temperature, slag velocity and slag thickness were the input parameters for the refractory brick corrosion model. Finally, the output of this model was the evolution of the brick thickness. Results showed that the external diffusion model could accurately predict the corrosion state with a good correlation coefficient using industry data. Furthermore, the slag shear rate on the surface of the refractory brick was a key control parameter for corrosion, especially for a top single-burner down-flow gasifier.

4.4 Corrosion of MgO-C refractory

Wang et al. [17] proposed a computational framework to represent the slag corrosion behaviours of the MgO-C refractory. A dynamic corrosion experiment using a rotating immersion approach was carried out to measure the material corrosion rate (**Figure 6**). Using this data, the overall corrosion activation energy was calculated based on the Arrhenius law. In the sequence, the flow pattern and thermal profile have been studied using a transient 3D numerical model of the dynamic corrosion experiment using a rotating immersion approach. The computational fluid dynamics developed model considered a domain including only the molten slag, but not the solid refractory. The continuity and time-averaged Navier–Stokes equations were invoked to describe the turbulent flow of the molten slag and the energy transport equation was solved to determine the heat transfer. Corrosion was considered in the form of transfer of MgO in the MgO-C refractory to the molten slag. The convection and diffusion of MgO in the

molten slag also promoted the dissolution of the MgO. These phenomena were expressed by the mass transport equation where the dissolution of MgO was represented as a source term defined by the Arrhenius law.

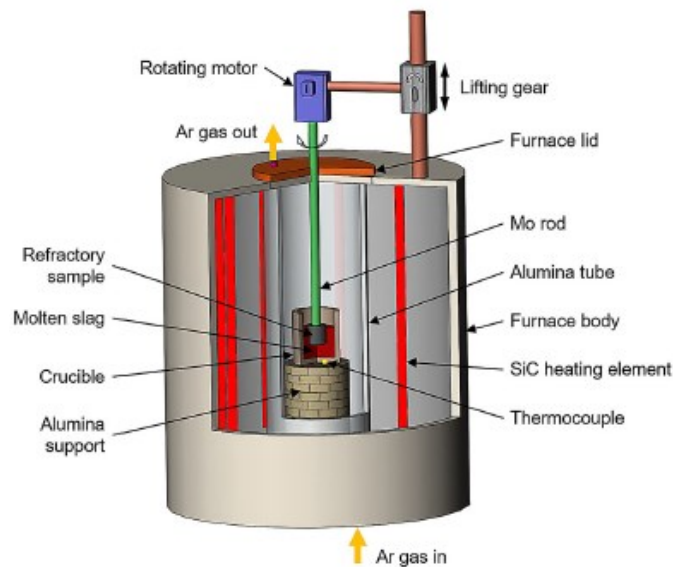


Figure 6: Schematics of the experimental set up [17].

In addition to the chemical reaction, the refractory corrosion behaviour was also considered to be affected by the wall shear stress, generating another expression for the corrosion rate. The general-purpose commercial software, ANSYS-FLUENT 18.2, was employed to complete the simulation. The governing equations for fluid flow, temperature profile, and component transport were integrated over each control volume and solved simultaneously using an iterative procedure. An illustration of the results of flow pattern and temperature from the model is presented in **Figure 7**.

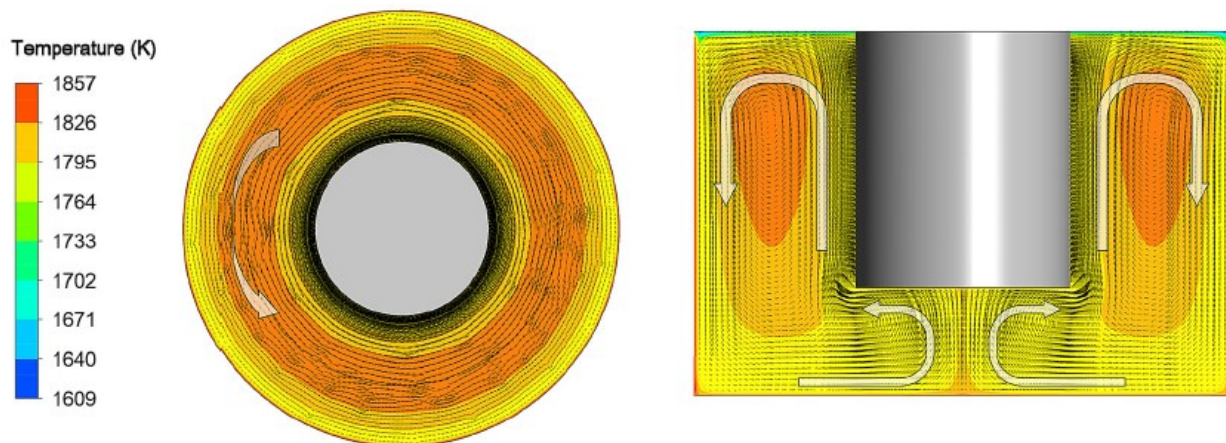


Figure 7: Distributions of flow pattern and temperature in the molten slag modelled through CFD[17].

Finally, a relationship was proposed to calculate the corrosion rate based on the wall shear stress, slag viscosity, sample size, overall corrosion activation, and difference in MgO content. The effect of the speed of rotation on the corrosion rate of the MgO-C refractory was then investigated using the numerical model and the proposed expression.

4.5 Model of a black liquor gasifier

In an approach more related to the design and behaviour of the general structure containing the refractory linings, Liang et al. [18] studied the failure behaviour of the refractory lining of black liquor gasifiers under chemical and thermomechanical loading by using an analytical model (**Figure 8**). The model is composed of two layers of refractory lining, one layer of fibre and finally the steel shell. Because of axisymmetry, each layer of refractory lining consists of only one-half of a brick. One side of the half brick model is the centreline of the brick and the other side corresponds to the brick joint as shown in **Figure 8b**. Since dry joints are used in the model, the brick joint will open under tensile stress.

The search for refractory materials for the lining of the black liquor gasifiers is complex since the combination of high temperature and alkalinity produces an aggressive environment for the reactor lining. Additionally, severe refractory thinning tends to occur

and several bricks can be found lost from the upper part of the gasifier vessel during operation. Furthermore, the refractory lining is subjected to the penetration of sodium and subsequent reactions with alkali-rich molten smelt, such that the refractory undergoes significant volume change and strength degradation. Thus, to accelerate the development of new refractory materials, computer simulation was used to model existing materials, as it is less costly and time-consuming than experimental studies.

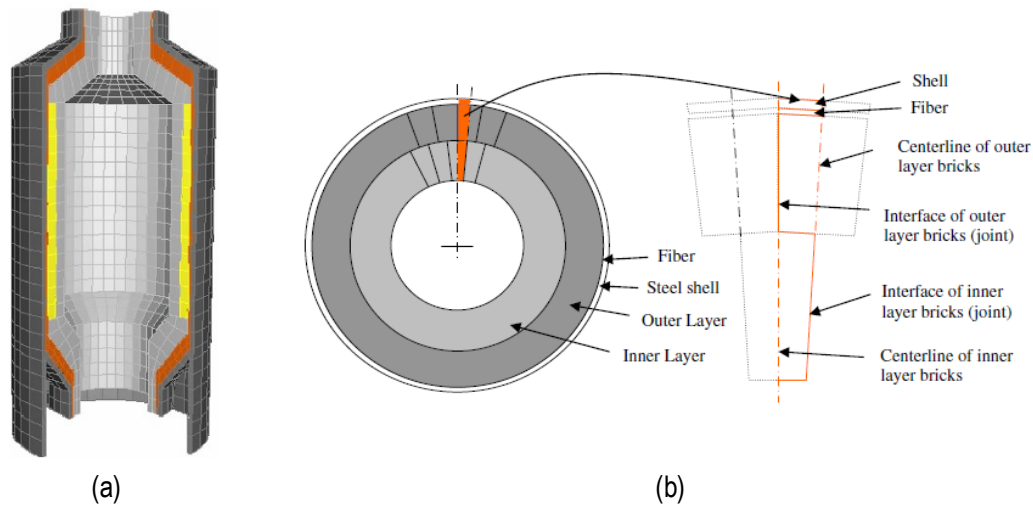


Figure 8: Blackliquor gasifier [18]; (a) Schematic construction of the black liquor gasifier, (b) Illustration of the modelled section.

A model based on continuum damage mechanics, accounting for the chemical expansion in addition to mechanical and thermal expansion, was presented to analyse the failure behaviour of the gasifier refractory lining under high temperature and chemically reactive environments by using the finite element method. The model was formed by the combination of non-associated, multi-hardening plasticity and isotropic damaged elasticity to describe the irreversible damage that occurs during the fracturing process, in which the dominant failure mechanisms are tensile cracking and compressive crushing of the refractory material. Due to the ductile behaviour of refractory at high temperature and the irreversible reactive strain due to the chemical attack, the plastic strain and chemical reactive strain were also included in the analysis in addition to the elastic strain. The chemical reaction is assumed to be continuous and linearly related to temperature and time. The reactive behaviour of the refractory material was expressed by the reactive strain which is proportional to temperature and time. Commercial finite element software Abaqus is used for the modelling.

In this study, due to lack of information regarding this topic, the chemical reaction was considered in form of a decrease in compressive and tensile strength. The numerical simulations and subsequent comparison of predicted damage patterns for black liquor gasifiers refractory material with the observed damage pattern in a glass melting furnace refractory brick indicated that this model could be used to evaluate the failure behaviour of refractory linings in black liquor gasifier. It was also shown that the chemical reaction was the cause for most compressive damage in the refractory structure and that layered damage occurred in the refractory structure due to the tensile damage. Moreover, it was observed that expansion allowance affects the damage of the refractory structure: tensile damage could be reduced by allowing for larger expansion and compressive damage was not dependent on the expansion allowance provided by the fibre layer. However, it is important to note that at the time this work was developed, no systematic experimental work had been done to characterise the failure of black liquor gasifiers. This work's final, and very important contribution, was the inclusion of a strain component representing the damage due to corrosion and showing its relevance for the final results.

4.6 Application of thermodynamics of irreversible processes for corrosion

Blond et al. [19],[20] used a model based on the thermodynamics of continuous porous media to investigate the effect of slag impregnation on thermal degradations. The proposed model was developed for quasi-brittle-impregnated refractories, which gives a closed-form solution for the maximum pressure in use, its location, and the thermal stresses. The authors showed the impact of the diffusivity ratio, the frequency, and the amplitude of the thermal history on the pressure amplitude as well as its maximum location. Some simplifications applied to the model were:

1. The liquid and skeleton were assumed to be chemically inert since, within an impregnated zone, the slag saturates chemically in the microstructure.
2. The liquid phase was assumed to be a homogeneous phase in the impregnated zone. Hence, the possible transformations at temperatures around 1200 °C were not taken into account.

3. Porosity was assumed to be a constant with depth.
4. The working lining was modelled as a one-dimensional half-space.
5. None-linear fracture (creep or plasticity) was not accounted for, and elastic properties (Young's modulus and Poisson's ratio, thermal expansion coefficient) were assumed to be temperature-independent.
6. A harmonic surface temperature was described on the free surface as:

$$\theta(0, t) = \theta_{max} \cos(\omega t + \phi) \quad \text{Equation 31}$$

Where θ_{max} is the temperature amplitude and ω is the frequency of the thermal loading. It should be mentioned that the loading history could be helpful for one to realize the role of cyclic load on the behaviour of the liquid that is present in the porous wall.

Two equations were solved to calculate the pressure $P(x, t)$. First, the diffusion equation or heat transfer was solved with Fourier's law. In the sequence, the liquid transfer with Darcy's law equation was solved; thermal diffusivity D_T and hydraulic conductivity k , were used respectively to characterise them. The problem was reduced to a pressure diffusion equation, which was written for the one-dimensional setting as:

$$\frac{\partial^2 P(x, t)}{\partial x^2} - \frac{1}{D_H} \frac{\partial P(x, t)}{\partial t} = \frac{\delta_v D_T}{k} \delta^2 \theta(x, t) \quad \text{Equation 32}$$

Where $\theta(x, t)$ is the temperature variation and D_H the hydraulic diffusivity; δ_v defines the relative bulk expansion variation between the pores and the saturating liquid. The authors considered δ_v equal to $-9.5 \times 10^{-6} K^{-1}$ and proposed a new solution with the suitable boundary conditions from which is shown in **Equation 33**:

$$P(x, t) = -\frac{\mu^2}{1 - \mu^2} \frac{P_{nd}}{\theta_{max}} [\theta(x, t) - \theta(\mu x, t)] \quad \text{Equation 33}$$

Where **Equation 34** is the field temperature, solution of the thermal diffusion equation with suitable boundary conditions.

$$\theta(x, t) = \theta_{max} e^{-x/L_c} \cos\left(\omega t - \frac{x}{L_c} + \phi\right) \quad \text{Equation 34}$$

The diffusivity ratio D_r and the characteristic length L_c are defined by

$$D_r = \frac{D_H}{D_T} \quad \text{Equation 35}$$

$$L_c = \sqrt{\frac{2D_T}{\omega}} \quad \text{Equation 36}$$

Undrained pressure (P_{nd}) was defined as "slag pressure" in closed pores filled by liquid, subjected to a temperature variation of amplitude θ_{max} as:

$$P_{nd} = -\delta_v \left(\frac{1}{M} + \frac{b^2}{3aK_o} \right)^{-1} \theta_{max} \quad \text{Equation 37}$$

The authors said that the maximum pressure P_{max} applies at the x_{cr} position during heating. At this stage, it is difficult to estimate the slag's damage pressure. However, the slag's pressure becomes negative during the cooling process, that may cause the slag suction, void nucleation, or both. Therefore, **Equation 38** was proposed in which half-space was considered to be a harmonic thermal loading, with a frequency ω , and a critical dimensionless abscissa X_{cr} , characterized by the ratio of the real critical length x_{cr} to the characteristic length L_c ($X_{cr} = x_{cr} / L_c$), was defined. In **Error! Reference source not found.** the only determinant parameter is μ .

$$e^{-(1-\mu)X_{cr}} + \mu e^{(1-\mu)X_{cr}} = (1 - \mu) \cos[(1 - \mu)X_{cr}] + (1 - \mu) \sin[(1 - \mu)X_{cr}] \quad \text{Equation 38}$$

The location of the maximum pressure P_{max} depends on the material parameter μ and the thermal loading frequency ω . According to the studies realized by the authors, the length of pressure peak could be written as:

$$L_c = \sqrt{2D_T t} \quad \text{Equation 39}$$

And the maximum pressure would be defined as proportional to the undrained pressure, which is proportional to the thermal amplitude:

$$\frac{P_{max}}{P_{nd}} = \left| \frac{\mu^2}{1 - \mu^2} \right| e^{(1-\mu)X_{cr}} \times \sqrt{1 + e^{-2(1-\mu)X_{cr}} \cos^2[(1 - \mu)X_{cr}]} \quad \text{Equation 40}$$

Using the thermoelasticity equation of porous-saturated media [21], the slag pressure was used to calculate the stress of the half-space. The normal stress which is perpendicular to the free surface σ_1 could be written as:

$$\sigma_1(x, t) = 0 \quad \text{Equation 41}$$

And the normal stresses, σ_2^{eff} and σ_3^{eff} , parallel to the free surface could be considered as:

$$\sigma_2^{eff}(x, t) = \sigma_3^{eff}(x, t) = \left(\frac{-2\mu_L}{\lambda_{Lo} + 2\lambda_L} \right) [bP(x, t) + 3\alpha_o K_o \theta(x, t)] \quad \text{Equation 42}$$

Where b is Biot's coefficient, λ_{Lo} and λ_L are Lamé's coefficient of the skeleton. The effective normal stresses applied to the skeleton e_i^{eff} could be written as:

$$e_i^{eff}(x, t) = \sigma_i(x, t) + bP(x, t) i = \{1, 2, 3\} \quad \text{Equation 43}$$

Combining **Equation 41** and **Equation 43** shows that the effective stress is proportional to the slag pressure. As a result, its extreme value is obtained at the same position and moment as the slag pressure. Whenever the pressure is positive, the skeleton is exposed to tensile stress responsible for opening the cracks parallel to the free surface. The effective normal stress for σ_2^{eff} and σ_3^{eff} could be obtained by combining the **Equation 42** and **Equation 43**.

$$\sigma_2^{eff}(x, t) = \sigma_3^{eff}(x, t) = \left(\frac{-1}{1 - v_0} \right) [v_0 bP(x, t) + \alpha_o E_o \theta(x, t)] \quad \text{Equation 44}$$

It was concluded that normal stress (σ_2^{eff} and σ_3^{eff}) is a combination of two parts. The first is a stress induced by the slag pressure and second a thermal stress induced by the thermal expansion of the skeleton and the magnitude of each part depends on the diffusivity ratio.

In another study De Bilbao et al. [22] studied the reactive impregnation of Al_2O_3 -CaO slag into porous high alumina refractory by performing the wicking test to test the transport properties of the porous media. Glycerine was used to simulate the non-reactive liquid impregnation, and the model developed to simulate transport considered mass and momentum conservation. According to the assumption applied, which was based on Darcy flow, the saturation could be written as:

$$\Phi \cdot \frac{\partial s}{\partial t} = \text{div} \left(\frac{K_{int}}{\mu} \Psi(s) \frac{\partial P_{cap}}{\partial s} \nabla s \right) \quad \text{Equation 45}$$

Where the saturation s is the ratio of liquid volume filling the porous space over porous volume, Φ is the porosity, and μ is the dynamic viscosity. The flow rate was defined using the intrinsic permeability K_{int} and relative permeability $\Psi(s)$. The capillary pressure P_{cap} was used to describe the state function of the liquid saturation s which the authors stated that according to the van Genuchten model [23], could be expressed as:

$$P_{cap}(s) = P_0 \left(S^{\frac{1}{m}} - 1 \right)^m \quad \text{Equation 46}$$

Where P_0 is a pressure reference and m an empirical parameter related to pore-size distribution.

Silicon carbide-based refractory castables (SiC-RC) were studied by Merzouki et al. [24]. In the paper, macroscopic constitutive equations were proposed to model the complex relationship between stress, strain, temperature, and oxidizing atmosphere in porous SiC-RC. To model the kinetics of the chemical swelling, oxygen content in the porosity of the heterogeneous material was estimated. The oxygen content was considered to depend on both the oxidation reaction of SiC-based grains and the diffusion of oxygen through the connected porosity in the castable. The multi-physical model was implemented in the finite element software Abaqus. It accounted for heat transfer, reactive oxygen transport, and chemically induced strain. A validation test was carried out on a cylindrical sample subjected to high temperatures with a thermal gradient in ambient air. Comparison between experimental results, observations and numerical results showed that the model provided a good description of the main physical phenomena.

Silicon-carbide based refractory castables (SiC-RC) are prime candidates for many industrial applications involving severe conditions. This is due to their outstanding mechanical properties, compared to other oxide refractories, and high thermal conductivity, which improves the heat transfer when the shield is a part of a heat exchanger. Additionally, SiC-RC have good resistance to corrosion and oxidation. However, when used as a protective lining in waste-to-energy plants, they progressively corrode with the production of new phases. Corrosion of SiC-RC in this situation involves complex mechanisms with several multiple chemical reactions depending on the nature of chemical species in the fluid, on the temperature and the transport properties across the lining. It does not necessarily lead to a deterioration of the mechanical properties of the SiC based refractory, but can induce a swelling that is responsible for additional stresses and may lead to failure of tiles.

In the work proposed by Merzouki et al. [24], attention was focused on the modelling of one corrosion mechanism in SiC-RC, namely the local passive oxidation of SiC particles. This choice was justified by the fact that this reaction is present in many high temperature applications. The proposed model included several phenomena, notably transport of oxygen by diffusion in the gas mixture, through the porosity and the induced overall chemical swelling.

The first part of the paper described the material and the main dry oxidation mechanisms. In addition, experiments to describe the isothermal oxidation behaviour and the oxidation under quasi-permanent thermal gradient were proposed. The experimental characterization of the oxidation behaviour of the SiC-RC was based on isothermal thermogravimetric analysis (TGA) and dilatometric analysis (DA). It was completed with an original experimental test of oxidation performed on a cylindrical sample subjected to a thermal gradient during two months. Experimental results were enriched with scanning electron microscope (SEM) observations and energy-dispersive X-ray spectroscopy (EDS) analyses.

The second part detailed the governing equations of the multi-physics model, the simplifications made and the identification of some parameters. The macroscopic thermo-chemo-mechanical model was built in the classical framework of thermodynamics of irreversible processes (TIP) applied to open continuous reactive media. The balance equations (mass, momentum, energy) and the constitutive equations (state laws and evolution laws), form the basis of this framework ensuring consistency of the model. The equations were written at a local macroscopic scale meaning that a representative volume element (RVE) of the SiC-RC exists and that macroscopic variables can be defined at the RVE scale. Additionally, the macroscopic balance and constitutive equations can be linked to the microscopic equations by averaging techniques. The mass balance was applied for each species contained in the unit volume of RVE in presence of the chemical reactions. The momentum balance was applied to the porous material to describe the motion of the different constituents, i.e. solid skeleton and gas mixture, in the RVE, and the energy balance equation was written for the reactive porous material. Furthermore, the set of constitutive equations of the problem composed of state laws (defined for each phase) and evolution laws, including heat conduction, chemical diffusion, oxidation kinetics, porosity evolution, and strain behaviour was presented.

The numerical simulations were made with the finite element software Abaqus. The computations have been performed in three successive steps to solve the set of constitutive and balance equations developed, as they are partially uncoupled. First, the heat transfer equations were solved, then the equations governing reactive gas transport through the porosity under thermal gradient, and lastly the mechanical problem, accounting for mechanical behaviour (homogeneous isotropic elasticity), temperature field, and oxidation extent field (inducing chemical expansion). User-supplied models were used to perform the reactive transport computation, and to define the thermal and chemical strains.

The developed model was validated through a numerical simulation of the experimental oxidation test of the cylindrical sample subjected to thermal gradient for 56 days. An axisymmetrical model was considered for the finite element analysis (Figure 9: Experimental set-up for the oxidation test under thermal gradient [24]). The proposed thermo-chemo-mechanical model gave an appropriate description of physical phenomena since a rather good agreement was obtained with SEM observations and macroscopic measurements. Such results validated the ability of the model to reasonably predict the swelling induced by the oxidation of part made of a SiC based refractory castable.

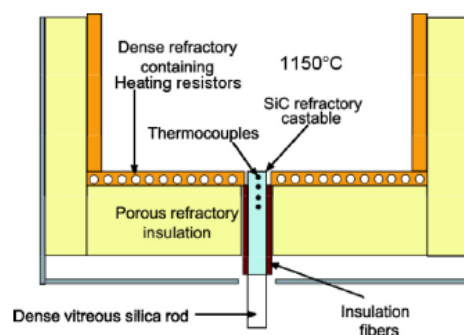


Figure 9: Experimental set-up for the oxidation test under thermal gradient [24].

In the following work, Blond et al. [25] reintroduced the irreversible thermodynamics framework to underline the implications of some basic thermodynamic concepts in terms of refractory behaviour modelling. The case of the degradation of oxide bonded SiC-based refractory used in Waste-To-Energy facilities (WTE) was once again used to illustrate the concepts and highlight the relevance of such an approach.

In WTE, a refractory lining protects the metallic water wall, which allows maximum recovery of heat from hot ashes and gases resulting from the burning of waste, against corrosion at high temperatures. One side of the refractory lining is in contact with the metallic water wall at a temperature of approximately 250 °C, and the other is in contact with smoke and ashes. The temperature in the combustion chamber varies from 500 °C to 1200 °C. The environmental conditions in the combustion chamber are difficult

to foresee because the nature and content of fumes and ashes depend on the waste burned and the incinerator process. Thus, numerous mechanisms of corrosion might be involved in the chemical degradation of the SiC-based refractory. At a macroscopic scale, the degradation of the refractory layer depends on both the material and the geometry of tiles. Progressive swelling of the material during service is a common mechanism observed in different plants with the result that stresses that can locally lead to rupture are introduced. In Blond et al. [25], the attention was exclusively focused on the oxidation of SiC as that is the first step of the degradation mechanism and it often participates to the degradation of SiC-based refractory structures. Finally, this choice simplified the illustration of the thermodynamics framework, allowing the authors to couple thermochemistry and thermomechanics with only one chemical reaction involved.

The first important step toward the creation of the macroscopic model was to define the representative elementary volume (REV) to be considered. Due to the characteristics of the commercial SiC-based refractory used, the REV was chosen to be close to 1 cm³. At this scale, this material can be viewed as an open, reactive, multiphasic, heterogeneous, deformable medium exchanging mass, heat, and work with its environment. It can be modelled as a continuous homogeneous porous multi-phasic medium. In this medium, the different phases are assumed to be superimposed at each point.

After defining the REV, it was essential to correctly identify the state variables to describe the behaviour of the system. This approach simplifies drawing of the physics in presence and their interactions and permits to not forget a coupling effect. In the application treated there, the physics taken into account were: heat transfer, mechanics, chemistry (i.e. SiC oxidation), and diffusion (i.e. oxygen flux through the gas into the porosity). The good state variables should be the temperature (easier to use than the entropy, even if it is not an extensive variable), the strain (for the mechanical state), the oxygen partial pressure in fumes/gas (playing a role in diffusion) and extent of oxidation. Once the state variables were defined, it was possible to write the local balance laws of the system: the heat equation, and the momentum and mass balance equation. The thermo-mechanical response of the material usually encompasses the state laws and the evolution laws of the material. In the case study, the behaviour was described by a linear elastic law and thermal strain. The swelling induced by corrosion was described by an evolution law of the mechanical state variable which depended on the chemical state variable (extent).

The proposed model was implemented using Abaqus software with the native laws together with the definition of user-supplied models. The model was validated by performing a numerical simulation of an experimental oxidation test of a SiC based castable cylinder subjected to an axial thermal gradient from room temperature to 1100 °C for 56 days. The main goals were to validate the expansion law and the temperature effect on oxidation extent. The main results are summarised in **Figure 10** and show that the variation in diameter all along the cylinder predicted by the numerical simulation is in agreement with the one obtained experimentally after 56 days (see the graph **Figure 10**). At the left, the final shape, the final radial displacement, and the extreme of temperatures during oxidation are represented.

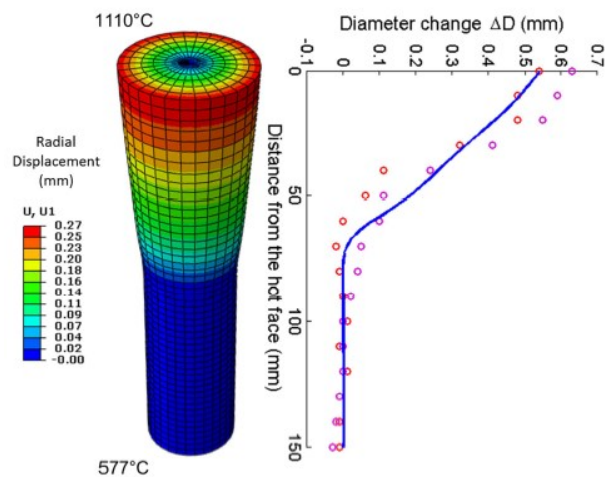


Figure 10: Experimental results and model prediction for long-term oxidation under thermal gradient. The blue curve represents numerical results, while red and violet points are experimental measurements along two perpendicular diameters [25].

Finally, to show the potential of prediction of in-service behaviour of refractory systems with such a model, two geometries of lining tiles have been modelled. The results presented show that the thermo-chemo-elasticity permitted the anticipation of both the effects of oxidation and geometry on mechanical stress. Then, the crack patterns observed on real SiC-based refractory tiles from the WTE plant could be anticipated. Such computations show that it becomes possible to refine the prediction of the stress localisation accounting for corrosion, and so to envisage the capacity to obtain reasonable lifespan prediction and improve the design of refractory linings in the future.

5 Conclusion

The development of physically meaningful multi-physics models in the refractory field requires a background in different fields of science, such as thermo-chemistry, thermal and mechanical analysis, as well as a solid understanding of mathematics. To implement the models for the computers to solve a numerical computational knowledge is essential. This report focused on the presentation of a mathematical framework capable of coupling the effects and consequently the equations related to each field of science to provide a solid basis for the development of numerical studies. Furthermore, some applications of numerical modelling of corrosion were shown. From the state-of-art works presented, it is clear that, although there exists a complete framework to study the coupled problem of thermo-chemo-mechanical behaviour of refractories, many of the studies recently developed still do not apply these types of concepts. Instead, the localized description of corrosion is targeted. Alternatively, Liang et al. [18] aims to describe the general response of the refractory structure [18], but does not describe in detail the evolution of corrosion. Lastly, the work developed by Blond et al. [19], [20], [25] and, Merzouki et al. [24] shows the application of TIP and how this framework is able to unify the description of the thermo-chemo-mechanical problem.

This growing field of research represents the future for the numerical study of refractory structures. With each passing day more realistic predictions are necessary to aid the design of refractory structures, assure that safety conditions are met, and ensure that the service lifetime is maximised. Thus, the application of multi-physics studies will enable industries to become more efficient and reduce their environmental impact.

6 References

- [1] C. Schacht, *Refractories handbook*. 2004.
- [2] J. Poirier, J. Smith, I. Jung, and Y. Kang, *Corrosion of Refractories: The Fundamentals*, vol. 2. 2017.
- [3] J. P. Bennett and J. D. Smith, *Fundamentals of Refractory Technology*. 2001.
- [4] H. . Uhlig and R. . Revie, "Uhlig's Corrosion Handbook," p. 1296, 2013.
- [5] R. A. McCauley and R. A. McCauley, "Corrosion of Ceramic and Composite Materials," *Corros. Ceram. Compos. Mater.*, Jun. 2004, doi: 10.1201/9780824752729.
- [6] P. N. Sudha, K. Sangeetha, A. V. Jisha Kumari, N. Vanisri, and K. Rani, *Corrosion of ceramic materials*, no. February. Elsevier Ltd., 2018.
- [7] J. Lemaitre and J.-L. Chaboche, *Mechanics of solid materials*. Cambridge university press, 1994.
- [8] S. Carnot, "Réflexions sur la puissance motrice du feu et sur les machines propres à développer cette puissance," in *Annales scientifiques de l'École Normale Supérieure*, 1872, vol. 1, pp. 393–457.
- [9] I. Prigogine, *Introduction to thermodynamics of irreversible processes*, 3d ed. New York: Interscience Publishers, 1968.
- [10] M. Pourbaix, "Thermodynamics and Corrosion," pp. 1–30, 1991, doi: 10.1007/978-94-011-3636-5_1.
- [11] T. Nishikawa, H. Todoriki, H. Itoh, and R. Kuroda, "Development of Numerical Prediction Model of Refractory Corrosion for Glass Melting Tank," 2005.
- [12] B. Zhang, J. Jin, and H. Liu, "Modeling Study of the Slag Behaviors and SiC Refractory Wall Corrosion on the Top Cone of a Membrane Wall Entrained-Flow Gasifier," 2020, doi: 10.1021/acs.energyfuels.0c02477.
- [13] K. Lin, Z. Shen, Q. Liang, J. Xu, and H. Liu, "Modelling of slag flow and prediction of corrosion state of refractory bricks in an entrained-flow gasifier," *Fuel*, vol. 275, p. 117979, Sep. 2020, doi: 10.1016/J.FUEL.2020.117979.
- [14] Q. Huang, P. Paul, D. Bhattacharyya, R. C. Pillai, K. Sabolsky, and E. M. Sabolsky, "Estimations of Gasifier Wall Temperature and Extent of Slag Penetration Using a Refractory Brick with Embedded Sensors," *Ind. Eng. Chem. Res.*, vol. 56, no. 35, pp. 9858–9867, Sep. 2017, doi: 10.1021/ACS.IECR.7B02604/SUPPL_FILE/IE7B02604_SI_001.PDF.
- [15] V. Muñoz, S. Camelli, and A. G. Tomba Martinez, "Slag corrosion of alumina-magnesia-carbon refractory bricks: Experimental data and thermodynamic simulation," *Ceram. Int.*, vol. 43, no. 5, pp. 4562–4569, Apr. 2017, doi: 10.1016/J.CERAMINT.2016.12.114.
- [16] T. K. Kaneko, J. P. Bennett, and S. Sridhar, "Effect of Temperature Gradient on Industrial Gasifier Coal Slag Infiltration into Alumina Refractory," *J. Am. Ceram. Soc.*, vol. 94, no. 12, pp. 4507–4515, Dec. 2011, doi: 10.1111/J.1551-2916.2011.04782.X.
- [17] Q. Wang, F. Tan, Z. He, G. Li, and J. Li, "Quantitative Evaluation of Slag Corrosion on MgO-C Refractory by Experimental and Numerical Simulation," *JOM*, vol. 73, no. 9, pp. 2709–2714, 2021, doi: 10.1007/s11837-021-04793-w.

- [18] X. Liang, W. L. Headrick, L. R. Dharani, and S. Zhao, "Modeling of failure in a high temperature black liquor gasifier refractory lining," *Eng. Fail. Anal.*, vol. 7, no. 14, pp. 1233–1244, Oct. 2007, doi: 10.1016/J.ENGFAILANAL.2006.11.043.
- [19] E. Blond, N. Schmitt, F. Hild, P. Blumenfeld, and J. Poirier, "Effect of slag impregnation on thermal degradations in refractories," *J. Am. Ceram. Soc.*, vol. 90, no. 1, pp. 154–162, Jan. 2007, doi: 10.1111/J.1551-2916.2006.01348.X.
- [20] E. Blond, N. Schmitt, J. Poirier, E. Blond, N. Schmitt, and J. Poirier, "Multi-physical analysis for refractory's design. Case of slag impregnated refractory."
- [21] F.-J. Ulm and O. Coussy, "Modeling of Thermochemomechanical Couplings of Concrete at Early Ages," *J. Eng. Mech.*, vol. 121, no. 7, pp. 785–794, Jul. 1995, doi: 10.1061/(ASCE)0733-9399(1995)121:7(785).
- [22] E. de Bilbao, M. Dombrowski, N. Traon, T. Tonnesen, J. Poirier, and E. Blond, "Study of Reactive Impregnation and Phase Transformations during the Corrosion of High Alumina Refractories by Al₂O₃-CaO Slag," *Adv. Sci. Technol.*, vol. 92, pp. 264–271, Oct. 2014, doi: 10.4028/WWW.SCIENTIFIC.NET/AST.92.264.
- [23] M. T. van Genuchten, "A Closed-form Equation for Predicting the Hydraulic Conductivity of Unsaturated Soils," *Soil Sci. Soc. Am. J.*, vol. 44, no. 5, pp. 892–898, Sep. 1980, doi: 10.2136/SSSAJ1980.03615995004400050002X.
- [24] T. Merzouki, E. Blond, N. Schmitt, M. L. Bouchetou, T. Cutard, and A. Gasser, "Modelling of the swelling induced by oxidation in SiC-based refractory castables," *Mech. Mater.*, vol. 68, pp. 253–266, Jan. 2014, doi: 10.1016/J.MECHMAT.2013.09.001.
- [25] E. Blond, T. Merouki, N. Schmitt, E. de Bilbao, and A. Gasser, "Multiphysics Modelling Applied to Refractory Behaviour in Severe Environments," *Adv. Sci. Technol.*, vol. 92, pp. 301–309, Oct. 2014, doi: 10.4028/WWW.SCIENTIFIC.NET/AST.92.301.